Thermodynamically Leveraged Tandem Catalysis for Ester RC(O)O–R′ Bond Hydrogenolysis. Scope and Mechanism

Tracy L. Lohr,[†,‡] Zhi Li,[†,‡,||] Rajeev S. Assary,[¶] Larry A. Curtiss,[¶] and Tobin J. Marks[*,†]

[†]Department of Chemistry, Northwestern University, 2145 Sheridan Road, Evanston, Illinois 60208, United States
[¶]Materials Science Division, Argonne National Laboratory, Argonne, Illinois 60439, United States

S *Supporting Information*

ABSTRACT: Rapid and selective formal hydrogenolysis of aliphatic ester RC(O)O–R′ linkages is achieved by a tandem homogeneous metal triflate + supported palladium catalytic system. The triflate catalyzes the mildly exothermic, turnover-limiting O–R′ cleavage process, whereas the exothermic hydrogenation of the intermediate alkene further drives the overall reaction to completion.


Thermodynamically leveraged tandem catalysis:
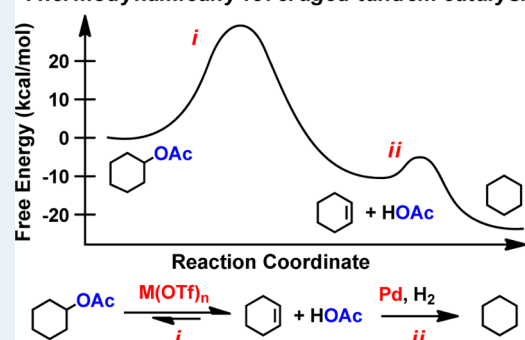
KEYWORDS: *C–O cleavage, biomass, tandem catalysis, thermodynamic leveraging, metal triflates, hydrogenolysis*

Ester functional groups are ubiquitous in nature as fat and oil components, and they represent one of the three major biomolecule classes along with carbohydrates and proteins. Esters are utilized extensively in products as diverse as motor fuels, polyesters, fine chemicals,[1a] and pharmaceuticals[1a–c] where they frequently serve as carboxylic acid protecting groups[1c–e] (e.g., Taxel and Cetraxate drugs).[1] For these reasons, new atom-efficient/greener means to cleanly catalyze ester modification processes are of great interest.

With respect to biomass, esters are most commonly found as triglycerides or fats, where the component long chain free fatty acids can be used for detergents, polymers, and surface coatings, and are an unconventional source of diesel fuel (biodiesel), which has attracted growing attention as an alternative to traditional petroleum-based fuels.[1g–i] Due to the widespread presence of triglycerides in biomass, efficient catalytic methods to break down esteric moieties for fuel or other chemicals via C–O bond cleavage processes, while also preserving the C3 functionality, are attractive. Although ester hydrolysis and transesterification are common, cleavage of esters to alkanes and carboxylic acids that is efficient, selective, and proceeds under nonaqueous/aprotic conditions, would be highly desirable.

A common characteristic of metal-catalyzed ester C_{alkoxy}–O cleavages is the requirement that the alkoxy (R′) group be either sp^2 hybridized or π-conjugated (allylic or benzylic).[2] There are also reports of ester C_{alkoxy}–O cleavage with nonconjugated aliphatic substituents, but these typically involve forcing decarboxylation conditions (250−500 °C) using noble metal/group 10 catalysts such as Pt,[3] Pd,[4] or Ni,[5] or high

temperature (400−500 °C) thermal cracking over zeolites or Al_2O_3 to afford CO_2 and the corresponding hydrocarbons (Figure 1).[6] Thus, there is currently a paucity of methodologies
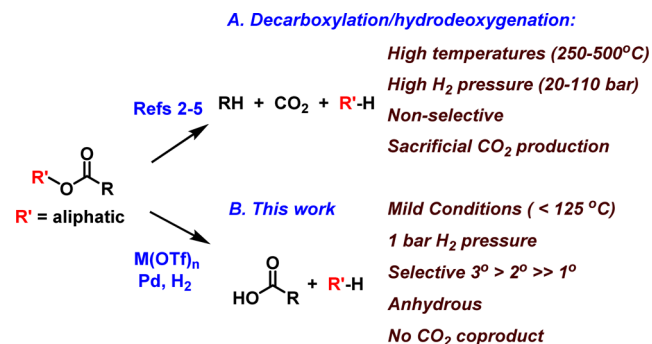
Figure 1. Comparison of decarboxylative and nondecarboxy-lative ester C–O hydrogenolysis processes.

for selective aliphatic ester C_{alkoxy}–O bond cleavage under mild conditions that avoids sacrificial decarboxylation processes.

Recently, our laboratory reported a thermodynamically leveraged, mechanism-based tandem strategy for the selective hydrogenolysis of diverse etheric C–O linkages.[7] The reactions are clean, selective, rapid, and mechanistically well-understood from both experiment and theory. These results raise the
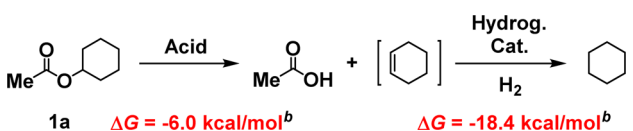
question of whether this approach might be generalizable to other biofeedstock oxygenates[8] and what might constitute the mechanistic constraints on those types of processes. Here we report a new transformation utilizing a tandem metal triflate Lewis acid + a heterogeneous Pd catalytic hydrogenation system that mediates rapid, selective, and clean ester C–O hydrogenolysis to the corresponding carboxylic acids and hydrocarbons (Figure 1, Table 1).

Table 1. Screening of Tandem Ester C–O Hydrogenolysis Catalysts and Conditions[a]

1a ΔG = -6.0 kcal/mol[b] ΔG = -18.4 kcal/mol[b]

	acid	hydrog. cat.	solvent	conv. (%)[c]	ρ[d]
1[e]	-	10% Pd/C	neat	N.R.	-
2[e]	La(OTf)₃	10% Pd/C	neat	N.R.	2.60
3[e]	Yb(OTf)₃	10% Pd/C	neat	N.R.	2.81
4[e]	Sc(OTf)₃	10% Pd/C	neat	N.R.	3.23
5	Ce(OTf)₄	10% Pd/C	neat	5	3.44
6	Fe(OTf)₃	10% Pd/C	neat	33	3.71
7	Al(OTf)₃	10% Pd/C	neat	56	3.87
8	Zr(OTf)₄	10% Pd/C	neat	56	4.29
9	Hf(OTf)₄	10% Pd/C	neat	89	4.37
10	HOTf	10% Pd/C	neat	20	-
11[e]	HOAc	10% Pd/C	neat	N.R.	-
12	Hf(OTf)₄	5% Pd/SiO₂	neat	85	4.37
13	Hf(OTf)₄	5% Pd/TiO₂	neat	74	4.37
14	Hf(OTf)₄	5% Pd/Al₂O₃	neat	31	4.37
15	Hf(OTf)₄	5% Pd/BaSO₄	neat	15	4.37
16	Hf(OTf)₄	5% Pt/C	neat	52	4.37
17[e]	Hf(OTf)₄	10% Pd/C	THF	N.R.	4.37
18[e]	Hf(OTf)₄	10% Pd/C	DMF	N.R.	4.37
19[e]	Hf(OTf)₄	10% Pd/C	MeOH	N.R.	4.37
20[e]	Hf(OTf)₄	10% Pd/C	H₂O	N.R.	4.37

[a]All reactions performed with 0.5 mol % acid catalyst, 0.2 mol % metal hydrogenation catalyst, under 1 bar of H₂ in neat substrate at 125 °C for 1 h unless otherwise noted. Volatile cyclohexane observed (*m/z* 84) by gas-phase MS. [b]DFT-computed free energy. [c]NMR conversion vs mesitylene internal standard. N.R. = no reaction. [d]ρ = DFT-computed effective metal ion charge density. [e]N.R. entries run for 4 h.

As shown in Table 1, DFT calculations indicate that both C–O bond cleavage and hydrogenation steps are thermodynamically favorable for the representative ester cyclohexyl acetate, **1a**. The elimination of acetic acid via C–O bond cleavage is computed to proceed with $\Delta G°$ = −6.0 kcal/mol, while cyclohexene hydrogenation proceeds with $\Delta G°$ = −18.4 kcal/mol.[9] Next, the effects of Lewis acid, hydrogenation catalyst, and solvent were investigated for the same model reaction, which cleanly gives acetic acid and cyclohexane as the only spectroscopically observable products (along with cyclohexene as an intermediate). Similar to ether hydrogenolysis,[7a,b,10] Lewis acid metal ions with high effective DFT-computed charge density (ρ) are most active, among which Hf(OTf)₄ exhibits the highest catalytic activity (entries 2–9, Table 1). Brønsted acids are not as effective (entries 10 and 11, Table 1). Pd/C and Pd/SiO₂ are similarly active as the hydrogenation component, outperforming other supported Pd catalysts (entries 12–16, Table 1). Coordinating solvents such as water and THF suppress the activity in comparison to the neat

substrate **1a** (entries 17−20, Table 1). To quantify product yields, Hf(OTf)₄ + Pd/C was run in neat **1a** at 125 °C for 2 h in a sealed glass vessel, before cooling in an ice bath. ¹H NMR spectroscopic analysis versus internal standard gives yields of 95% and 97% for cyclohexane and AcOH, respectively (with trace benzene; see Table S4 for AcOH yields).

The reaction mechanism was first probed via kinetic analysis, which shows that the CH₃C(O)O−cyclohexyl cleavage reaction is zero-order in substrate concentration, zero-order in H₂ pressure, and first-order in Lewis acid concentration (Figures S1−S5), yielding the rate law shown in eq 1. The

$$\upsilon = k[\text{substrate}]^0[\text{H}_2]^0[\text{Lewis acid}]^1 \qquad (1)$$

zero-order in substrate kinetics indicates that, under the conditions studied (0.5 mol % Lewis acid), the homogeneous metal triflate catalyst is operating under saturation kinetics. The RC(O)O−R′ cleavage event is reasonably turnover-limiting in this tandem scenario, as supported by the first-order dependence on metal triflate and the zero-order dependence on H₂ pressure. The overall reaction yields activation parameters of $\Delta H^{\ddagger}$ = 25(2) kcal mol⁻¹ and $\Delta S^{\ddagger}$ = −8(1) e.u., in an Eyring analysis (Table S1). The slightly negative $\Delta S^{\ddagger}$ indicates that the transition state is to some degree organized and polar, as might be anticipated from a Lewis acid-mediated charge separation event stabilized by secondary substrate molecules.

The extent to which the RC(O)O−R′ bond cleavage transition state involves some degree of charge separation[11] was further probed via acyl (R) substituent effects (Table 2).

Table 2. Influence of Carboxylate Substitution on RC(O)O−R′ Hydrogenolysis Activity[a]

	R−	conv. (%)[b]
1	CH₃−	89
2	CH₃CH₂−	60
3	(CH₃)₂CH-	42
4	(CH₃)₃C−	33
5[c]	CF₃−	100
6[c,d]	CF₃−	83
7	ClCH₂−	93
8	Cl₂CH₂−	61
9	Cl₃C−	44

[a]All reactions performed with 0.5 mol % Hf(OTf)₄, 0.2 mol % Pd/C (10% metal loading), under 1 bar of H₂ in neat substrate at 125 °C for 1 h unless otherwise noted. [b]NMR conversion vs mesitylene internal standard. [c]1,1,2,2-tetra-chloroethane used as internal standard to avoid Friedel−Crafts reaction with mesitylene. [d]Reaction time = 10 min.

Using cyclohexyl acetate as a benchmark, introducing successive methyl groups at the acetate β-carbon atom progressively depresses activity (entries 1−4, Table 2), suggesting that carboxylate steric bulk hinders carbonyl group activation by the metal triflate. Electronic effects were examined by substituting the acyl hydrogens with fluorine or chlorine moieties. Cyclohexyl trifluoroacetate is found to be far more reactive (entries 5 and 6, Table 2), while the first chlorine substitution slightly accelerates the cleavage rate (entry 7, Table 2) and successive chlorine additions slow the reaction rate (entries 7−9, Table 2), most likely due to increasing steric hindrance between the ester and triflate ligands on the Hf

center. Taken together, these results indicate that less basic, and nonsterically hindered carboxylates (e.g., CF_3COO^-) react most rapidly in this transformation.

The present catalytic hydrogenolysis is far more sensitive to alkoxy (R′) group identity (Table 3) than to that of the

Table 3. Alkoxy Group R′ Effects on Catalytic Ester Hydrogenolysis Activity[a]

	Substrate, 2	Products, 3/4	Temp (°C)	Time (h)	Conv. (Yield) (%)
1	n-C_8H_{17}OAc	$(n$-$C_8H_{17})_2$O $+ n$-C_8H_{18}	125	18	13 (3, 3) (4, 9)
2	n-C_8H_{17}OAc	n-C_8H_{18}	200	3.0	62 (59)
3	(structure) OAc	(structure)	125	1.0 / 18	16 / 78 (76)
4	(structure) AcO	(structures) 82 : 18	125	0.5	100 (89)
5	(structure) OAc	(structure) 2	125	18	~1 (1)
6	(structure) OAc	(structure)	125	1.0 / 18	12 / 100 (97)
7	PhCH$_2$OAc	oligomers	125	1.0	N.D.
8	PhCH$_2$CH$_2$OAc	PhCH$_2$CH$_3$	125	1.0 / 18	26 / 100 (76)
9	(structure) OAc Ph	PhCH$_2$CH$_3$	25	1.0 / 18	54 / 98 (97)
10	(structure) OAc	oligomers	125	1.0	N.D.
11[b]	(structure) OAc	(structure)	25	0.17	100 (-)
12	(structure) OAc OAc Ph	Ph (structure) OAc Ph (structure) OAc	25	18	36 (10) (19)

[a]All reactions performed with 0.5 mol % Hf(OTf)$_4$, 0.2 mol % Pd/C (10% metal loading), and 1 bar of H$_2$ in neat substrate at the temperature and for the time indicated. N.D. = not determined. Yields of products are shown in parentheses. Yields of AcOH are reported in Table S4. [b]AcOH (96% yield) and trace product detected in the liquid phase. Gas-phase MS showed both 2-methylbutane and 2-methyl-butene.

carboxylate group, likely reflecting the importance of stabilizing a carbocationic intermediate and/or partially charge-separated transition state. Under 1 bar of H$_2$ and 125 °C, the primary ester n-octyl acetate does not readily undergo RC(O)O−R′ hydrogenolysis. Instead, partial hydrolysis of the ester to acid and alcohol, and subsequent dehydration of the alcohol to ether (making the process catalytic in water) is observed (entry 1, Table 3). However, at 200 °C, n-octyl acetate undergoes acetic

acid elimination to alkene, which subsequently undergoes hydrogenation (entry 2, Table 3). Secondary esters are more readily cleaved to the desired alkane + acetic acid (entry 3, Table 3), while tertiary esters are the most reactive substrates (entry 4, Table 3). Although 1-adamantyl acetate undergoes RC(O)O−R′ hydrogenolysis to yield adamantane (entry 6, Table 3), 2-adamantyl acetate only undergoes slight hydrolysis/condensation to yield trace amounts of (2-adamantyl)$_2$O (entry 5, Table 3), presumably reflecting the inhibitory strain of olefin formation. We do not believe carbonyl hydrogenation to the alcohol is occurring, as entries 5 and 6 would then show similar reactivity. Regardless of the substitution order, benzylic and allylic esters are generally the most reactive. Devoid of β-H atoms, benzyl acetate reacts rapidly to afford oligomers (entry 7, Table 3). Esters with β-H atoms that facilitate styrene formation yield the desired hydrogenolysis products with higher efficiency, even at 25 °C (entries 8−9, Table 3). Finally, allyl esters are extremely reactive, and rapid cleavage ensues at 25 °C (entries 10−11, Table 3). These results suggest that ester RC(O)O−R′ hydrogenolysis activity tracks the stability of the corresponding R′ carbocations: tertiary > secondary ≫ primary. The yields in Table 3 indicate that ester hydrogenolysis, where feasible, is clean, with the majority of mass balances >90%.

Selectivity was further probed using 1,2-bis-acetoxy-2-phenylethane as a substrate (Table 3, entry 12), where the 2° benzylic ester cleaves preferentially over 1° cleavage. No 2-phenylethanol acetate is observed, indicating the 2° ester position is more reactive, and that reactivity trends for esters on the same molecule follow those of the individual esters. The conversion is low at room temperature, which may reflect chelation of Hf(OTf)$_4$ by both ester functionalities.

Applying this catalytic protocol to the biomass relevant triglyceride Tricaprylin (n-C_7H_{15} alkyl chains) at 200 °C/2 h achieves up to 96% conversion to C$_3$-based hydrocarbons, along with related 1,2, 1,3, and 1-oxygenates, as well as the n-C_7H_{15}C(O)OH fatty acid in high yields (see Table S5). C$_3$ product selectivity is highly dependent on conversion and conditions. Using less acidic M(OTf)$_n$ (M = Al, Ce) affords higher 1,2 and 1,3-oxygenate selectivity (up to 27 and 11%, respectively, Table S7), while Hf(OTf)$_4$ favors propane and the 1-oxygenate (up to 72 and 22%, respectively, Table S7). Addition of MeOH to the reaction mixture affords the corresponding methyl ester (biodiesel) from n-C_7H_{15}C(O)OH in quantitative yield.

To provide additional atomistic understanding of the pathway for Hf(OTf)$_4$-mediated cyclohexyl acetate hydrogenolysis, a detailed solution phase enthalpic profile was computed by DFT techniques (Figure 2, see Supporting Information). This profile includes the structures of all intermediates (**A** to **G**) along the reaction coordinate. All energies are with respect to that of isolated Hf(OTf)$_4$ and the substrate, denoted **A** (0.0 kcal/mol). From Figure 2 it can be seen that the most favorable catalyst−cyclohexyl acetate binding to occurs via the ester carbonyl group, and that the **A** → **B** process is exothermic by 23.4 kcal/mol—more so than binding via the etheric oxygen, which (not shown) is exothermic by ~12 kcal/mol. RC(O)O−R′ bond cleavage occurs via a transition state **C** (−8.1 kcal/mol) that requires an intrinsic barrier of 16.3 kcal/mol from **B**. The cleavage of the RC(O)O−R′ bond results in the formation of an intermediate **D** (−14.3 kcal/mol) containing a carboxylate ion coordinated in a bidentate fashion to the Hf(IV) ion, while the cyclohexyl
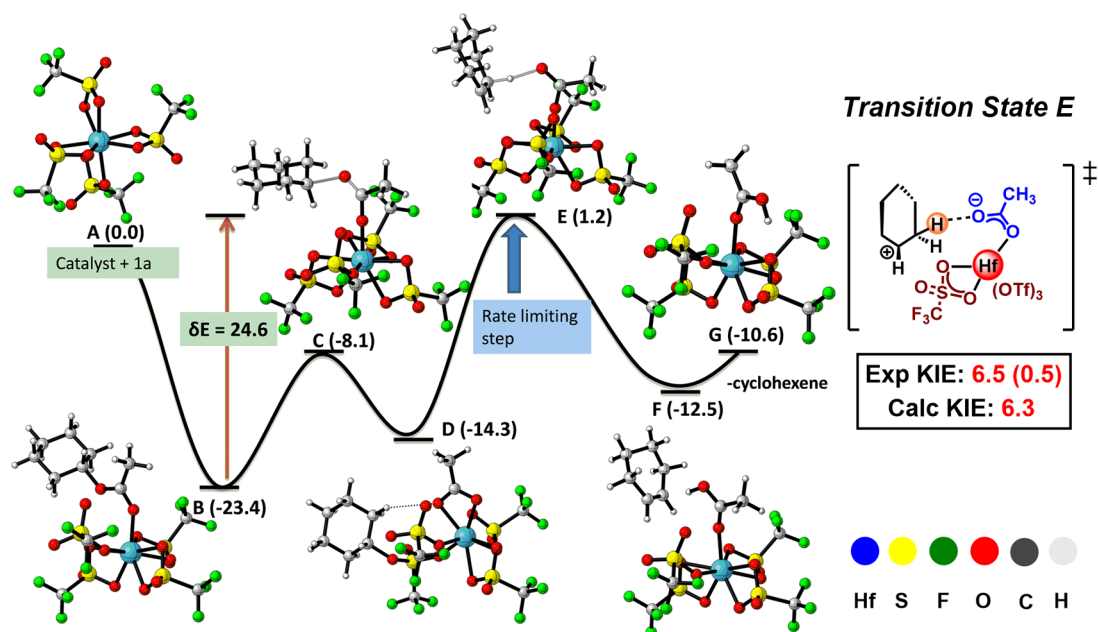
Figure 2. Calculated enthalpy profile (energies in kcal/mol) and rate-determining transition state for RC(O)O−R′ bond cleavage by Hf(OTf)$_4$ along with experimental and calculated KIE's.

cation is weakly stabilized via interaction with one of the triflate oxygens. Formation of cyclohexene and acetic acid (coordinated to Hf) occurs via transition state **E** (1.2 kcal/mol) with proton transfer from the cyclohexyl cationic moiety to the carboxylate anion. This process (**D → F**) via **E** is computed to be highest point in the enthalpy and free energy profiles (Table S7) and is likely the rate-controlling step of the reaction sequence. The calculated kinetic isotope effect (KIE) for this step is 6.3, in good agreement with the experimental KIE of 6.5 (0.5). The computed apparent enthalpy of activation using an *energy span* approach is 24.6 kcal/mol (ΔH(**E-B**)), in good accord with the experimental value of 25(2) kcal/mol.

In summary, hydrogenolytic ester C−O cleavage catalyzed by a tandem homogeneous metal triflate/supported Pd system exhibits a broad scope, including secondary and tertiary esters (≤125 °C) and primary esters (200 °C) at 1 bar of H$_2$, with the resulting products being alkanes and carboxylic acids. This result represents an atom economical, anhydrous, and most importantly, selective (allylic ≥ benzylic >3° > 2° ≫ 1°) approach to cleaving aliphatic ester RC(O)O−R′ functionalities at lower temperatures and pressures than traditional decarboxylative processes. The present tandem catalytic system also produces biodiesel from triglycerides in high yield without coproduction of undesired[12] glycerol. Instead, the C3 backbone is preserved and converted to hydrocarbons and/or oxygenates. Further mechanistic and computational analysis of this catalytic ester transformation will be reported in a future manuscript, along with a full account of triglyceride transformations.

ASSOCIATED CONTENT

Ⓢ Supporting Information

The Supporting Information is available free of charge on the ACS Publications website at DOI: 10.1021/acscatal.5b00950.

> Experimental details, substrate synthesis, characterization, kinetic plots for determining rate law, Eyring analysis plots, KIE experiments, error analysis, and computational details (PDF)

AUTHOR INFORMATION

Corresponding Author

*E-mail: t-marks@northwestern.edu.

Present Address

∥(Z.L.) ShanghaiTech University, 100 Haike Road, Pudong District, Shanghai 201210, China.

Author Contributions

‡These authors contributed equally (T.L.L. and Z.L.).

Notes

The authors declare no competing financial interest.

REFERENCES

(1) (a) Gunanathan, C.; Milstein, D. *Chem. Rev.* **2014**, *114*, 12024−12087. (b) Srivastava, R. S. *Appl. Organomet. Chem.* **1993**, *7*, 607. (c) Barbayianni, E.; Kokotos, G. *ChemCatChem* **2012**, *4*, 592−611.

(d) Corma, A.; Iborra, S.; Velty, A. *Chem. Rev.* **2007**, *107*, 2411−2502.
(e) Sartori, G.; Ballini, R.; Bigi, F.; Bosica, G.; Maggi, R.; Righi, P. *Chem. Rev.* **2003**, *104*, 199−250. (f) Guillier, F.; Orain, D.; Bradley, M. *Chem. Rev.* **2000**, *100*, 2091−2158. (g) Huber, G. W.; Iborra, S.; Corma, A. *Chem. Rev.* **2006**, *106*, 4044−4098. (h) Straathof, A. J. J. *Chem. Rev.* **2013**, *114*, 1871−1908. (i) Besson, M.; Gallezot, P.; Pinel, C. *Chem. Rev.* **2013**, *114*, 1827−1870.

(2) Juteau, H.; Gareau, Y. *Synth. Commun.* **1998**, *28*, 3795−3805.

(3) Madsen, A. T.; Ahmed, E.; Christensen, C. H.; Fehrmann, R.; Riisager, A. *Fuel* **2011**, *90*, 3433−3438.

(4) (a) Han, J.; Sun, H.; Ding, Y.; Lou, H.; Zheng, X. *Green Chem.* **2010**, *12*, 463−467. (b) Hollak, S. A. W.; Ariens, M. A.; de Jong, K. P.; van Es, D. S. *ChemSusChem* **2014**, *7*, 1057−1062. (c) Boda, L.; Gyorgy, O.; Solt, H.; Ferenc, L.; Valyon, J.; Thernesz, A. *Appl. Catal., A* **2010**, *374*, 158−169.

(5) (a) Wang, C. X.; Liu, Q. H.; Song, J.; Li, W.; Li, P.; Xu, R. S.; Ma, H. J.; Tian, Z. J. *Catal. Today* **2014**, *234*, 153−160. (b) Srifa, A.; Faungnawakij, K.; Itthibenchapong, V.; Viriya-Empikul, N.; Charinpanitkul, T.; Assabumrungrat, S. *Bioresour. Technol.* **2014**, *158*, 81−90. (c) Song, W. J.; Zhao, C.; Lercher, J. A. *Chem. - Eur. J.* **2013**, *19*, 9833−9842. (d) Santillan-Jimenez, E.; Morgan, T.; Lacny, J.; Mohapatra, S.; Crocker, M. *Fuel* **2013**, *103*, 1010−1017. (e) Liu, Q. Y.; Zuo, H. L.; Wang, T. J.; Ma, L. L.; Zhang, Q. *Appl. Catal., A* **2013**, *468*, 68−74. (f) Kandel, K.; Frederickson, C.; Smith, E. A.; Lee, Y. J.; Slowing, II *ACS Catal.* **2013**, *3*, 2750−2758. (g) Peng, B. X.; Yuan, X. G.; Zhao, C.; Lercher, J. A. *J. Am. Chem. Soc.* **2012**, *134*, 9400−9405. (h) Peng, B. X.; Yao, Y.; Zhao, C.; Lercher, J. A. *Angew. Chem., Int. Ed.* **2012**, *51*, 2072−2075. (i) Liu, Y. Y.; Sotelo-Boyas, R.; Murata, K.; Minowa, T.; Sakanishi, K. *Energy Fuels* **2011**, *25*, 4675−4685.

(6) (a) Kim, S. K.; Han, J. Y.; Lee, H. S.; Yum, T.; Kim, Y.; Kim, J. *Appl. Energy* **2014**, *116*, 199−205. (b) Zhao, C.; Bruck, T.; Lercher, J. A. *Green Chem.* **2013**, *15*, 1720−1739. (c) Gosselink, R. W.; Hollak, S. A. W.; Chang, S. W.; van Haveren, J.; de Jong, K. P.; Bitter, J. H.; van Es, D. S. *ChemSusChem* **2013**, *6*, 1576−1594. (d) Choudhary, T. V.; Phillips, C. B. *Appl. Catal., A* **2011**, *397*, 1−12. (e) Morgan, T.; Grubb, D.; Santillan-Jimenez, E.; Crocker, M. *Top. Catal.* **2010**, *53*, 820−829. (f) Smith, B.; Greenwell, H. C.; Whiting, A. *Energy Environ. Sci.* **2009**, *2*, 262−271. (g) Lestari, S.; Maki-Arvela, P.; Beltramini, J.; Lu, G. Q. M.; Murzin, D. Y. *ChemSusChem* **2009**, *2*, 1109−1119.

(7) (a) Atesin, A. C.; Ray, N. A.; Stair, P. C.; Marks, T. J. *J. Am. Chem. Soc.* **2012**, *134*, 14682−14685. (b) Assary, R. S.; Atesin, A. C.; Li, Z.; Curtiss, L. A.; Marks, T. J. *ACS Catal.* **2013**, *3*, 1908−1914. (c) Li, Z.; Assary, R. S.; Atesin, A. C.; Curtiss, L. A.; Marks, T. J. *J. Am. Chem. Soc.* **2014**, *136*, 104−107. (d) Lohr, T. L.; Marks, T. J. *Nat. Chem.* **2015**, in press. DOI: 10.1038/NCHEM.226.

(8) Sutton, A. D.; Waldie, F. D.; Wu, R. L.; Schlaf, M.; Silks, L. A.; Gordon, J. C. *Nat. Chem.* **2013**, *5*, 428−432.

(9) See SI for calculation details.

(10) Kundu, S.; Choi, J.; Wang, D. Y.; Choliy, Y.; Emge, T. J.; Krogh-Jespersen, K.; Goldman, A. S. *J. Am. Chem. Soc.* **2013**, *135*, 5127−5143.

(11) (a) Nitsch, D.; Huber, S. M.; Pöthig, A.; Narayanan, A.; Olah, G. A.; Prakash, G. K. S.; Bach, T. *J. Am. Chem. Soc.* **2014**, *136*, 2851−2857. (b) Davies, A. G.; Kenyon, J. *Q. Rev., Chem. Soc.* **1955**, *9*, 203.

(12) (a) Nakagawa, Y.; Tamura, M.; Tomishige, K. *J. Mater. Chem. A* **2014**, *2*, 6688−6702. and references therein. (b) Zhou, C. H.; Zhao, H.; Tong, D. S.; Wu, L. M.; Yu, W. H. *Catal. Rev.: Sci. Eng.* **2013**, *55*, 369−453. (c) Johnson, D. T.; Taconi, K. A. *Environ. Prog.* **2007**, *26*, 338−348. (d) Ayoub, M.; Abdullah, A. Z. *Renewable Sustainable Energy Rev.* **2012**, *16*, 2671−2686. (e) Lee, C. S.; Aroua, M. K.; Daud, W. M. A. W.; Cognet, P.; Peres-Lucchese, Y.; Fabre, P. L.; Reynes, O.; Latapie, L. *Renewable Sustainable Energy Rev.* **2015**, *42*, 963−972. (f) Varrone, C.; Liberatore, R.; Crescenzi, T.; Izzo, G.; Wang, A. *Appl. Energy* **2013**, *105*, 349−357. (g) Quispe, C. A. G.; Coronado, C. J. R.; Carvalho, J. A., Jr. *Renewable Sustainable Energy Rev.* **2013**, *27*, 475−493. (h) Le Tu, T.; Okitsu, K.; Luu Van, B.; Maeda, Y. *Catalysts* **2012**, *2*, 191−222.